Design and fabrication of broadband rugate filter*

Zhang Jun-Chao(张俊超)[a)b)], Fang Ming(方 明)[a)], Shao Yu-Chuan(邵宇川)[a)b)], Jin Yun-Xia(晋云霞)[a)], and He Hong-Bo(贺洪波)[a)†]

[a)] *Key Laboratory of Material Science and Technology for High Power Lasers, Shanghai Institute of Optics and Fine Mechanics, Chinese Academy of Sciences, Shanghai* 201800, *China*

[b)] *Optic and Laser Division, National Institute of Metrology, Beijing* 100013, *China*

(Received 16 August 2011; revised manuscript received 8 October 2011)

The design and the deposition of a rugate filter for broadband applications are discussed. The bandwidth is extended by increasing the rugate period continuously with depth. The width and the smoothness of the reflection band with the distribution of the periods are investigated. The improvement of the steepness of the stopband edges and the suppression of the side lobes in the transmission zone are realized by adding two apodized rugate structures with fixed periods at the external broadband rugate filter interfaces. The rapidly alternating deposition technology is used to fabricate a rugate filter sample. The measured transmission spectrum with a reflection bandwidth of approximately 505 nm is close to that of the designed broadband rugate filter except a transmittance peak in the stopband. Based on the analysis of the cross-sectional scanning electron microscopic image of the sample, it is found that the transmission peak is most likely to be caused by the instability of the deposition rate.

Keywords: rugate filter, broadband, rapidly alternating deposition

PACS: 42.79.Ci, 42.79.Ry, 81.15.Cd **DOI:** 10.1088/1674-1056/21/5/054219

1. Introduction

The rugate filter is a kind of gradient index optical thin film characterized by a continuous sinusoidal refractive index variation in the direction of the substrate normal.[1,2] The rugate filter has optical and mechanical properties that differ from those of discrete multilayer stacks, including efficient suppression of harmonics,[3] low stress,[4] higher scratch and wear resistance, and superior laser induced damage thresholds.[5] Many deposition processes, such as evaporation,[6−8] reactive sputtering,[9,10] glancing angle deposition,[11,12] and porous silicon (PS),[13] have been frequently used to prepare the gradient index coatings. The accuracy in controlling the refractive index variation is the main concern in the deposition processes of these available techniques.

In many applications, for example, passband, stopband, and edge filters, it is desirable to achieve reflectance over an extended spectral region.[14] Broadband filters can be realized by stacking many different periodic multilayer coatings[15] or using chirped structures.[16] However, the spectra of these structures usually present unwanted higher-order harmonic reflectance peaks outside the primary reflectance region.

In this paper, we design a broadband rugate filter by changing the sinusoidal period of the refractive index profile. In order to increase the steepness of the stopband edges, two apodized rugate structures with fixed periodicities are added to the boundaries of the broadband filter. The rapidly alternating deposition technology is used to fabricate the broadband rugate filter sample.

2. Design of broadband rugate filter

The refractive index profile of a rugate filter is usually expressed as

$$n(x) = n_{\rm a} + \frac{1}{2} n_{\rm p} \sin\left(\frac{2\pi x}{T} + \varphi_0\right), \qquad (1)$$

where $n_{\rm a}$ is the average refractive index, $n_{\rm p}$ is the peak-to-valley refractive index amplitude, φ_0 is the phase at the substrate in radians, and T is the period of the sine wave. The wavelength that spectrally locates the reflection band is determined by

$$\lambda_0 = 2T. \qquad (2)$$

*Project supported by the National Natural Science Foundation of China (Grant No. 10704079) and the NSAF Joint Fund, China (Grant No. 10976030).

†Corresponding author. E-mail: hbhe@siom.ac.cn

© 2012 Chinese Physical Society and IOP Publishing Ltd

The bandwidth of the stopband is given by[17]

$$B_{\mathrm{W}} = \frac{n_{\mathrm{p}}}{2n_{\mathrm{a}}}\lambda_0. \tag{3}$$

It is observed from Eq. (3) that the bandwidth can be enlarged by increasing refractive index contrast n_{p} or reducing average index n_{a}. However, the method is not optimal for the design of broadband filters because of the limitation of the available coating materials.

For the following design, the rugate period varies continuously throughout the filter as shown in Fig. 1. The total number of the rugate cycles is N. The rugate period changes from the maximum value ($T_{\max}$) to the minimum one ($T_{\min}$) in the form of

$$T_i = T_{\max} - (T_{\max} - T_{\min})\left(\frac{i-1}{N-1}\right)^{\alpha}, \tag{4}$$

where α is a parameter controlling the distribution of the periods. Any stopband of interest can be realized simply by selecting suitable $T_{\max}$ and $T_{\min}$.

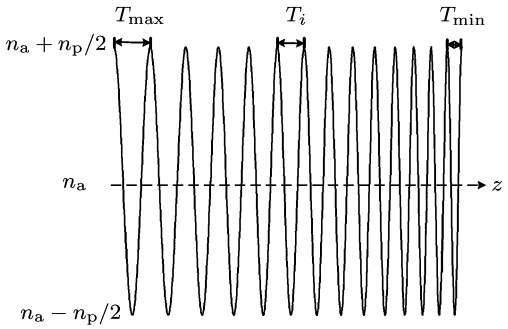


Fig. 1. Schematic diagram of the refractive-index profile of a broadband rugate structure.

In the following, we investigate how index α affects the reflectance spectrum. The substrate we used in the design is the BK7 glass ($n_{\mathrm{s}} = 1.52$), and the ambient medium is air ($n_0 = 1.0$). The other parameters are set to be $n_{\mathrm{a}} = 1.78$, $n_{\mathrm{p}} = 0.58$, $N = 50$, $T_{\max} = 550$ nm, and $T_{\min} = 350$ nm. Figure 2 shows the transmission spectra of the broadband rugate filters with $\alpha = 1.0$, 0.8, and 0.6 respectively. It is shown that with the decrease of α, the reflection band shifts toward the short wave and the bandwidth becomes smaller. The ripples in the shorter wavelength boundaries of the stopband are suppressed more and more obviously. However, the suppression effect becomes worse in the longer wavelength region. When $\alpha = 0.8$, the total region of high reflectance is relatively flat, and the bandwidth is very satisfactory. The smoothness and the optical density of the stopband can be improved further by increasing the total number of the periods. However, this comes at the expense of increasing the thickness of the film.

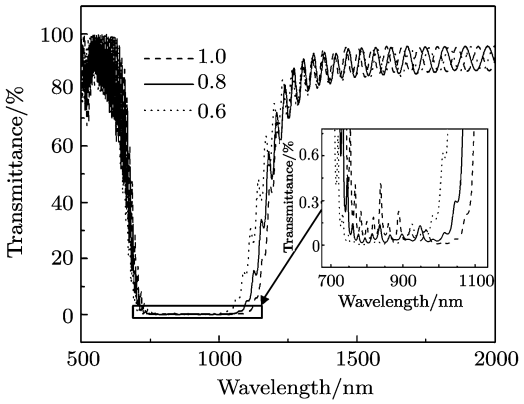


Fig. 2. Transmission spectra of rugate filters with different values of α. Inset shows the expansion of the reflection band.

Although the stopband is extended significantly as shown in Fig. 2, the transmittance curves present some defects, such as large side lobes in the transmission zones and small steepness of the stopband edge. We add two apodized simple rugate filters with fixed period lengths, whose corresponding frequencies are the same as the boundary frequencies of the broadband filter respectively to optimize the functionality of the broadband filter. Two quintic matching layers are adopted to reduce the ripples outside the reflection band. The refractive index profile of the modified broadband rugate filter is shown in Fig. 3. The central segment (A) is the chirped rugate structure with the number of the rugate cycles being 35. The number and the length of the cycles of the simple rugate section of fixed period (segment B_1) are 11 and 550 nm, respectively. The corresponding values of the other fixed period rugate structure (segment B_2) are 14 and 350 nm, respectively. The refractive index profiles of both segments are modulated by a quintic function, which is given by[18]

$$n(x) = n_{\mathrm{a}} + \frac{1}{2}n_{\mathrm{p}}f(x)\sin\left(\frac{2\pi x}{T}\right), \tag{5}$$

$$f(x) = 10x^3 - 15x^4 + 6x^5. \tag{6}$$

Two symmetrical segments (C_1 and C_2) with an optical thickness of 1 μm each are used as layers that match the substrate to the incident medium. The quintic matching profiles on both sides are limited by the lowest allowed refractive index (1.52).

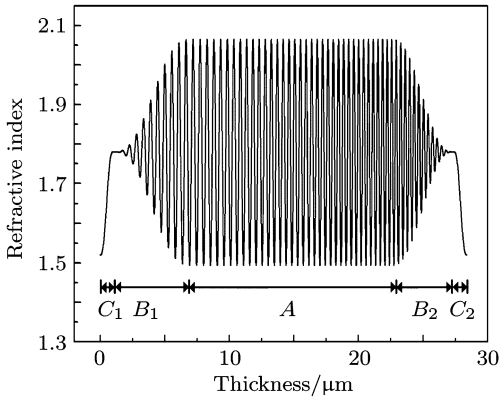


Fig. 3. Refractive index distribution of the modified broadband rugate filter.

3. Experiment

A broadband rugate filter was fabricated by pulsed direct-current (dc) magnetron sputtering at a base pressure of 1.0×10^{-3} Pa with rapidly alternating deposition.[19] The oxides Nb_2O_5 and SiO_2 of the metals were formed by a reactive process during the thin-film growth. The BK7 glass (30 mm×3 mm) substrates were ultrasonically cleaned in acetone and ethanol before being introduced into the vacuum system. During deposition, oxygen and argon were admitted to the process chamber with the same flow rate of 20 sccm, and the pressure was maintained at 0.5 Pa.

In order to simplify the experimental process, we let the powers of Nb ($P_{\rm Nb}$) and Si ($P_{\rm Si}$) targets satisfy the following formula:

$$P_{\rm Nb} + 2.5 \times P_{\rm Si} = 1.05 \text{ kW}. \quad (7)$$

The cross-sectional microstructure was observed by using field emission scanning electron microscopy (SEM) with a Zeiss Auriga microscope. The transmission spectra of the coatings were measured by a Lambda 900 spectrophotometer in the 500 nm to 2000 nm spectral range.

4. Results and discussion

Figure 4 shows the refractive indices and the physical thicknesses of the composite films, which were fabricated in equal intervals of time (85 min) with different values of $P_{\rm Nb}$. The fitted polynomial expressions are

$$\begin{aligned} n(P_{\rm Nb}) &= 1.4782 + 0.32127 \times P_{\rm Nb} \\ &\quad + 0.28615 \times P_{\rm Nb}^2 + 0.29866 \times P_{\rm Nb}^3, \quad (8) \\ d(P_{\rm Nb}) &= 397.959 - 234.891 \times P_{\rm Nb} \\ &\quad + 106.295 \times P_{\rm Nb}^2 + 131.482 \times P_{\rm Nb}^3. \quad (9) \end{aligned}$$

It is clear that at wavelength $\lambda = 900$ nm, the effective refractive index of composite $(Nb_2O_5)_{1-x}(SiO_2)_x$ thin film changes from 1.49 to 2.07.

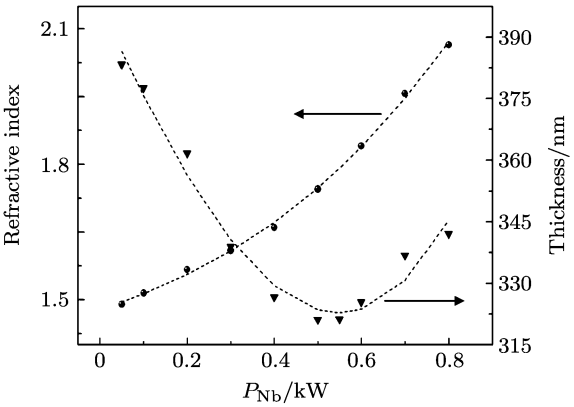


Fig. 4. Fitted refractive index at $\lambda = 900$ nm and physical thickness of Nb_2O_5–SiO_2 composite film each as a function of the power of the Nb target.

Based on the above parameters, a broadband rugate filter with a refractive index profile shown in Fig. 3 was fabricated. The measured and the calculated transmission spectra are shown in Fig. 5. It can be found that the experimental result is similar to the theoretical design. The measured full width at half maximum (FWHM) of the stopband is approximately 505 nm. There is a noteworthy difference between them, i.e., a transmission peak with a maximum transmittance of 10.3% appears in the measured reflection band.

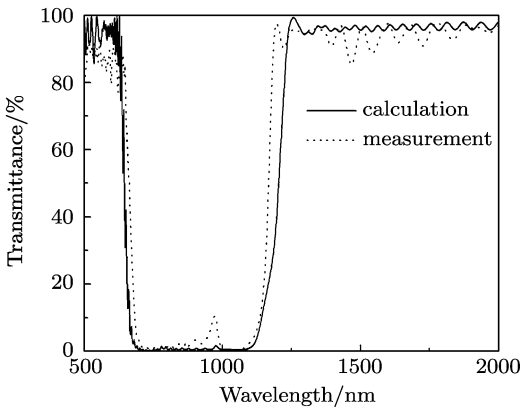


Fig. 5. Transmission spectra of theoretical calculation and experimental measurement for the broadband filter.

In order to analyze the difference, the cross-sectional image of the sample was investigated by SEM, as shown in Fig. 6. The white (dark) region corresponds to the layer with a higher (lower) percentage

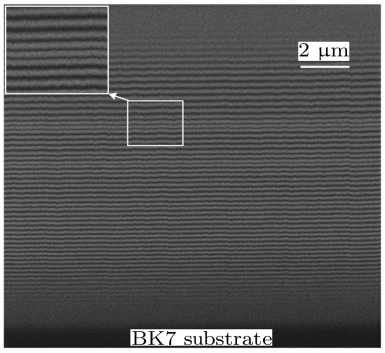


Fig. 6. SEM cross-sectional image of the filter.

of Nb_2O_5. The intensity variation in the film represents the refractive index gradient. The boundary regions with low contrast are the matching and the apodization layers. It is clear that the period length decreases from the air side to the substrate side. However, a defect consisting of about three cycles, whose periods are narrower than the normal values, is seen in the inset. The refractive indexes of this defect layer range from about 1.55 to 2.09, as derived from the SEM micrograph. The defect might be due to the instability of the deposition rate of SiO_2 in this region, which leads to a smaller thickness and a larger refractive index of the composite film. A simulated transmission spectrum of a broadband rugate filter with a defect is depicted in Fig. 7. As can be seen, in the spectrum

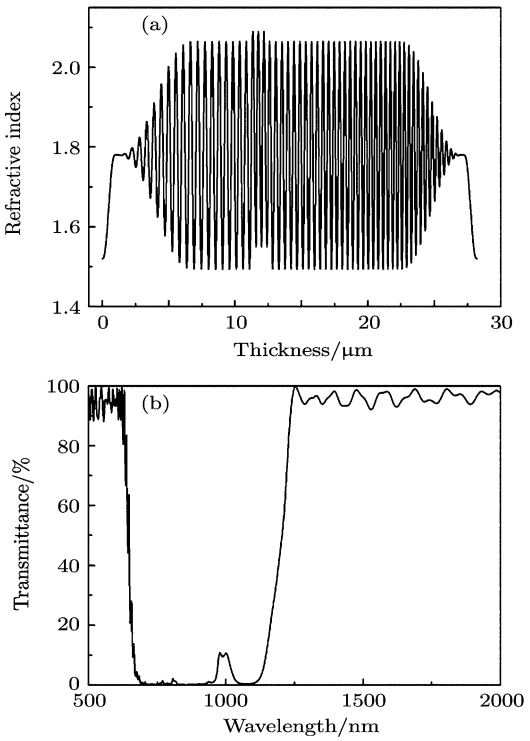


Fig. 7. (a) Refractive-index profile, (b) simulated transmission spectrum of a broadband rugate filter with a defect.

there is a transmittance peak in the stopband region, which is similar to the one shown in Fig. 5.

5. Conclusion

We present a new method to design a broadband rugate filter by continuously varying the cycle periods of the sinusoidal refractive index profile. The width and the position of the reflection band can be adjusted by selecting different external periods. Two rugate structures (using quintic apodization) with fixed period lengths, whose corresponding frequencies are the same as the boundary frequencies of the broadband filter, are adopted to increase the steepness of the stopband edge and suppress the side lobes on both sides of the stopband.

Composite $(Nb_2O_5)_{1-x}(SiO_2)_x$ thin films are fabricated by using the rapidly alternating deposition technology. The refractive index and the deposition rate of the composite film each as a function of the sputtering power of Nb (Si) are investigated. The experimental transmission spectrum is accordant with the calculated result except a transmission peak inside the stopband. The measured full width at half maximum of the stopband is about 505 nm. The microstructure of the filter is observed by SEM. By simulating the spectrum of a rugate filter with a defect, we find that the deposition rate instability may cause the transmission peak.

References

[1] Zhao L, Sui Z, Zhu Q H, Zhang Y and Zuo Y L 2009 *Acta Phys. Sin.* **58** 3977 (in Chinese)
[2] Bovard B G 1993 *Appl. Opt.* **32** 5427
[3] Baumeister P W 1985 *Appl. Opt.* **24** 2687
[4] Tang C J, Jaing C C, Lee K S and Lee C C 2008 *Appl. Opt.* **47** C167
[5] Jupé M, Lappschies M, Jensen L, Starke K and Ristau D 2007 *SPIE* 640311
[6] Shen Z C, Wang Y J, Fan Z X and Shao J D 2005 *Acta Phys. Sin.* **54** 0295 (in Chinese)
[7] Gunning W J, Hall R L, Woodberry F J, Southwell W H and Gluck N S 1989 *Appl. Opt.* **28** 2945
[8] Tsai R Y and Hua M Y 1996 *Appl. Opt.* **35** 5073
[9] Shen Z C, Shao J D, Wang Y J and Fan Z X 2005 *Acta Phys. Sin.* **54** 4842 (in Chinese)
[10] Bartzsch H, Lange S, Frach P and Goedicke K 2004 *Surf. Coat. Technol.* **180–181** 616
[11] Shen Z C, Shao J D, Wang Y J and Fan Z X 2005 *Acta Phys. Sin.* **54** 3069 (in Chinese)
[12] Kong W J, Shen Z C, Wang S H, Shao J D, Fan Z X and Lu C J 2010 *Chin. Phys.* B **19** 044210
[13] Berger M G, Arens-Fischer R, Thönissen M, Krüger M, Billat S, Lüth H, Hilbrich S, Theiß W and Grosse P 1997 *Thin Solid Films* **297** 237

[14] Ishikura N, Fujii M, Nishida K, Hayashi S, Diener J, Mizuhata M and Deki S 2008 *Opt. Mat.* **31** 102

[15] Agarwal V and Río J A 2003 *Appl. Phys. Lett.* **82** 1512

[16] Bruyant A, Lérondel G, Reece P J and Gal M 2003 *Appl. Phys. Lett.* **82** 3227

[17] Abu-Safia H A, Al-Sharif A I and Abu Aljarayesh I O 1993 *Appl. Opt.* **32** 4831

[18] Lee C C, Tang C J and Wu J Y 2006 *Appl. Opt.* **45** 1333

[19] Zhang J C, Fang M, Shao Y C, Jin Y X and He H B 2011 *Chin. Phys.* B **20** 094212